Two gustatory receptors involved in host plant recognition of silkworm larvae

Haruka Endo[1,2,4,5,*], Kana Tsuneto[2,4], Takayuki Yamagishi[2], Dingze Mang[2,6], Katsuhiko Ito[3], Shinji Nagata[1] and Ryoichi Sato[2,*]

[1]Department of Integrated Bioscience, Graduate School of Frontier Sciences, The University of Tokyo, Kashiwa, Chiba 277-8562, Japan

[2]Graduate School of Bio-Applications and Systems Engineering, Tokyo University of Agriculture and Technology, Koganei, Tokyo 184-8588, Japan

[3]Department of Science of Biological Production, Graduate School of Agriculture, Tokyo University of Agriculture and Technology, Fuchu,Tokyo 183-8509, Japan

[4]The authors contributed equally.

[5]Present address: RIKEN Center for Brain Science, 2-1 Hirosawa, Wako, Saitama 351-0198, Japan

[6]Present address: College of Life Science, Institute of Life Science and Green Development, Hebei University, Baoding 071002, China

*Correspondence: haruka.endo@riken.jp (H.E.) or ryoichi@cc.tuat.ac.jp (R.S.).

Abstract

Herbivorous insects can identify their host plants by sensing plant secondary metabolites as chemical cues. We previously reported the two-factor host acceptance system of the silkworm *Bombyx mori* larvae. The chemosensory neurons in the maxillary palp (MP) of the larvae detect mulberry secondary metabolites, chlorogenic acid (CGA), and isoquercitrin (ISQ), with ultrahigh sensitivity, for host plant recognition and feeding initiation. Nevertheless, the molecular basis for the ultrasensitive sensing of these compounds remains unknown. In this study, we demonstrated that two gustatory receptors (Grs), BmGr6 and BmGr9, are responsible for sensing the mulberry compounds with attomolar sensitivity for host plant recognition by silkworm larvae. Calcium imaging assay using cultured cells expressing the silkworm putative sugar receptors (BmGr4-10) revealed that BmGr6 and BmGr9 serve as receptors for CGA and ISQ with attomolar sensitivity in human embryonic kidney 293T cells. CRISPR/Cas9-mediated knockout (KO) of BmGr6 and BmGr9 resulted in a low probability of making a test bite of the mulberry leaves, suggesting that they lost the ability to recognize host leaves specifically. Electrophysiological recordings showed that the loss of host recognition ability in the Gr-KO strains was due to a drastic decrease in MP sensitivity toward ISQ in BmGr6-KO larvae and toward CGA and ISQ in BmGr9-KO larvae. Our findings unraveled that the two Grs, which have been regarded as sugar receptors, are molecules responsible for detecting plant phenolics in host plant recognition.

Keywords: herbivorous insects, host-plant selection, plant secondary metabolites; silkworm; gustatory receptors

Introduction

Herbivorous insects and plants have evolved through reciprocal adaptation. Plants have various physical and chemical defense mechanisms to combat insect herbivory [1]. For instance, plants have evolved a variety of secondary metabolites, most of which act as feeding deterrents and are often toxic to herbivorous insects [2]. In turn, herbivorous insects have adapted to some of the chemicals by developing chemosensory systems, enzymatic detoxication, and other mechanisms, which enabled them to consume a specific limited range of plants [3,4]. In parallel, they were able to identify host plants using plant secondary metabolites as sensory cues [5].

Sensory exploration at the leaf surface is essential for host plant selection in larval feeding and adult ovipositioning [6,7]. We previously reported that the silkworm *Bombyx mori* larvae, well known for their preference for mulberry leaves, feed on the leaves utilizing a two-factor authentication system controlled by two taste organs and a set of chemoreceptors with differing sensitivities, operating sequentially in time [8]. The first step involves probing the leaf surface with the maxillary palp (MP), which contains ultrasensitive chemosensory neurons sensitive to a set of crucial mulberry compounds, including secondary metabolites (chlorogenic acid [CGA] and quercetin glycosides) and a phytosterol (β-sitosterol). The ultrahigh sensitivities in the attomolar and femtomolar ranges enable the larvae to detect trace amounts of these compounds at the dry leaf surface [6,9] and identify the host leaves. If these three compounds are detected simultaneously, the larva makes a test bite, which leads to the second step. Another gustatory organ, the maxillary galea (MG), is used to probe the sugar content released by the test bite. Sucrose mainly induces continued biting, resulting in feeding. The two-factor host acceptance system is expected to be conserved among herbivorous insects because of their typical stepwise feeding behavior, composed of foraging, palpation at the leaf edge, test and persistent biting, and swallowing [10,11]. Although understanding the behavioral and neural basis of host acceptance in silkworm larvae has progressed, the molecular basis underlying MP's ultrasensitive detection of the mulberry compounds remains unknown.

Insects have three prominent chemosensory receptor families: gustatory (Grs), olfactory (Ors), and ionotropic receptors (Irs) [12]. Most Grs and some Irs are believed to mediate taste. Research on insect chemosensory receptors is advanced in the fruit fly, *Drosophila melanogaster*. *Drosophila* Gr5a and Gr64a-f are broad-tuned sugar receptors [13–15]. *Drosophila* Gr43a and its orthologs in other insect species have been reported as fructose-specific receptors [16,17], whereas some lepidopteran Grs in the same lineage respond to *myo*-inositol [18,19]. Some Grs in *Drosophila* are receptors for toxic compounds, including plant secondary metabolites [20], but many of these "bitter" Grs do not have clear ortholog relationships across insect orders. Some Irs were reported to detect amino acids and fatty acids in *Drosophila* [21,22].

Some Grs have been reported as receptors for plant secondary metabolites in lepidopteran insects. PxutGr1 from the swallowtail butterfly, *Papilio xuthus*, is responsible for the sensitivity of tarsal taste sensilla to synephrine, which acts as an ovipositioning stimulant [23]. PrapGr28 from the cabbage butterfly, *Pieris rapae*, contributes to sinigrin sensitivity in adult tarsal taste sensilla [24], although sinigrin is a feeding stimulant for their larvae [25]. PxylGr34 from the diamondback moth, *Plutella xylostella*, is involved in response to canonical plant hormones, brassinolide, and 24-epibrassinolide, a feeding and oviposition deterrent, in MG of larvae [26]. BmGr16, BmGr18, and BmGr53 from *B. mori* respond to coumarin and caffeine in human embryonic kidney 293T (HEK293T) cells [27], but their role *in vivo* is unknown. The two Ors in *P. xylostella*, Or35 and Or49, are necessary and sufficient for detecting isothiocyanates, which act as ovipositioning stimulants and its host cruciferous plants [28]. Thus, several examples of low-sensitive chemoreceptors for plant secondary metabolites in the foreleg of adult and MG of larvae have been reported. However, ultrahigh-sensitive chemoreceptors in larval MP underlying the first step in the two-factor host acceptance system are unknown.

We addressed the molecular basis of host recognition in silkworm larvae in the present study. *In vitro* calcium imaging in the cells suggested that BmGr6 and BmGr9 are candidates that confer MP ultrahigh sensitivity for CGA and ISQ. CRISPR/Cas9-mediated KOs demonstrate that the two Grs are responsible for host recognition by sensing CGA and/or ISQ.

Results

BmGr6 and BmGr9 serve as ultrahigh-sensitive receptors for CGA and ISQ in HEK293T cells and sugar receptors

We started with phylogenetic analysis to find closely related silkworm Grs with PxutGr1, a candidate receptor for CGA and ISQ because PxutGr1 is the only Gr reported as a receptor for plant phenolics [23]. Phylogenetic analysis of lepidopteran Grs indicates that PxutGr1 belongs to the same lineage as BmGr9 and BmGr10, *Drosophila* Gr43a orthologs in the silkworm (Fig. 1). Based on the phylogenetic analysis, we focused on BmGr9 and BmGr10 in the Gr43a clade, and BmGr4-8 in the neighboring putative sugar receptor clade [29].

To test whether these seven Grs can confer silkworm MP chemosensory neurons attomolar sensitivity to CGA and ISQ, we performed calcium imaging in HEK293T cells. Of the seven Grs-expressing cells, BmGr6-, BmGr8-, and BmGr9-expressing cells responded to 100 aM CGA, and BmGr6- and BmGr9-expressing cells responded to 100 aM ISQ (Fig. 2A-C). We recorded a dose-dependent response of BmGr6, BmGr8, BmGr9, and BmGr10 (Fig. 2D and E) and determined the EC_{50} values (Table S1). Although BmGr6- and BmGr9-expressing cells responded to <10 aM CGA and ISQ, BmGr8-expressing cells did not respond to 10 aM CGA (Fig. 2D). Based on these results, we focused on and further characterized BmGr6 and BmGr9 as candidates conferring MP neurons attomolar sensitivities toward CGA and ISQ. BmGr6- and BmGr9-expressing cells did not respond to β-sitosterol up to 2 μM (Fig. S1).

112 Since BmGr6 is regarded as a putative sugar receptor [29] and BmGr9 was reported as a fructose
113 receptor [16], we investigated their response to major sugars present in the mulberry leaves (D-
114 fructose, D-glucose, sucrose, and *myo*-inositol) [19]. Surprisingly, BmGr9-expressing cells responded
115 to D-fructose with aM sensitivity (Fig. 2C and D), whereas they exhibited relatively lower sensitivities
116 to D-glucose, sucrose, and *myo*-inositol (Fig. 2E and F). BmGr6-expressing cells showed pM to nM
117 sensitivity to four sugars (Fig. 2C-F). These results indicate that the two Grs are highly tuned to CGA
118 and ISQ, whereas BmGr9 also exhibits a high affinity with D-fructose.
119
120 **BmGr6 and BmGr9 are expressed in subsets of MP chemosensory neurons**
121 According to the RNA-seq data from a previous study, BmGr6 and BmGr9 are highly expressed in
122 the MP [30]. To confirm this at the protein level, we performed immunohistochemistry using anti-
123 BmGr6 and anti-BmGr9 antisera. Each sensillum in MP contains three to five chemosensory neurons
124 whose somas are usually clustered in the second segment (Fig. 3A and 3B) [31]. We observed three
125 BmGr6-antiserum-positive MP neurons (Fig. 3C). In the two representative cryosections, two of the
126 three neurons are close to each other (Fig. 3C), suggesting that the two neurons are contained in the
127 same sensillum. We observed seven BmGr9-antiserum-positive MP neurons, three of which are close
128 to each other (Fig. 3D). Thus, BmGr6 and BmGr9 are expressed in at least three and seven neurons
129 in the MP of silkworm larvae.
130
131 **BmGr6-KO and BmGr9-KO larvae lose their ability to recognize mulberry leaves specifically**
132 To test whether the two Grs are involved in host recognition *in vivo*, we generated BmGr6-KO and
133 BmGr9-KO silkworm strains via the CRISPR/Cas9 system. We designed single-guide RNAs
134 (sgRNAs) targeting the exons 5 and 3 of the *BmGr6* and *BmGr9* genes (Fig. 4A). By injecting the
135 sgRNAs and the Cas9 protein into eggs, we successfully established mutant strains carrying
136 homozygous null mutations of *BmGr6* and *BmGr9* (material and methods for details). In both strains,
137 premature stop codons were generated via indel mutations (Fig. 4A and S2).
138 The body mass of the fifth instar larvae of BmGr6-KO and BmGr9-KO strains, which have been fed
139 with artificial diets since hatching, were ~86% and ~91% of the body mass of wild-type (WT) larvae
140 (Fig. 4B). First, we conducted 1.5 h short-term feeding assay using artificial diets and mulberry leaves.
141 When feeding on leaves, the larvae must recognize host leaves by MP to initiate feeding (the first
142 step of the host acceptance system) [8]. This step can be skipped when feeding artificial diets with
143 abundant sugars on their surface are available. The feeding amount of artificial diets by BmGr6-KO
144 larvae was ~85% of the WT larvae (Fig. 4C), suggesting that the low body mass of BmGr6-KO larvae
145 is due to the low feeding amount of artificial diets. The feeding amount of BmGr9-KO larvae is
146 comparable with that of WT (Fig. 4C), suggesting that factors that affect long-term feeding, such as
147 the interval of feeding, are involved in the low body mass of BmGr9-KO larvae. The feeding amounts
148 of mulberry leaves by the two mutant larvae were significantly lower than the WT (Fig. 4D). To directly
149 observe the ability of host recognition, we next observed test bites toward mulberry leaves. Only 33%

150 and 35% of BmGr6-KO and BmGr9-KO larvae made test bites within 1 min, whereas 90% of WT
151 larvae made test bites (Fig. 4E). This low probability of test biting corresponds to those of some
152 nonhost leaves in WT larvae [8], suggesting that the two mutant strains lose their ability to recognize
153 mulberry leaves. Even when BmGr6-KO and BmGr9-KO larvae were making test bites within 1 min,
154 and their palpation time until making a first test bite was significantly longer than that of WT larvae
155 (Fig. 4F), suggesting that even if mutant larvae made a test bite, they were not able to recognize
156 mulberry leaves immediately. These results indicate that BmGr6 and BmGr9 are essential for host
157 recognition *in vivo*.
158
159 **BmGr6 and BmGr9 are responsible for sensing ISQ and both CGA and ISQ, respectively: *in***
160 ***vivo***
161 We performed electrophysiological recordings from MP to test whether the two Grs are involved in
162 CGA and ISQ sensing *in vivo*. The MP neurons of BmGr6-KO larvae started responding to CGA from
163 10 aM and showed almost the same sensitivity as WT larvae (Fig. 5A and B); they did not respond to
164 ISQ up to 1 μM (Fig. 5A and C). This suggests that the ISQ sensitivity of BmGr6-KO larvae was $>10^{10}$-
165 fold lower than the MP neurons of WT larvae. By contrast, both CGA and ISQ sensitivities of BmGr9-
166 KO larvae were ~1,000-fold lower than those of WT larvae (Fig. 5A-C), suggesting that BmGr9 is
167 required for attomolar sensitivities of both CGA and ISQ. We previously reported that the β-sitosterol
168 sensitivity of MP neurons is at the femtomolar level [8]. The number of spikes toward 10 fM β-sitosterol
169 was comparable between WT, BmGr6-KO, and BmGr9-KO strains (Fig. S3), suggesting that MP of
170 the two mutant strains preserved the sensitivity to β-sitosterol. BmGr6 and BmGr9 are required for
171 the attomolar sensitivity to ISQ, and BmGr9 is required for attomolar sensitivity to CGA; nevertheless,
172 BmGr6 is not involved in CGA sensing *in vivo*. Unlike *in vitro* study observations in Fig. 2, these results
173 indicate different roles of BmGr6 and BmGr9 *in vivo*.
174
175 **Discussion**
176 **Functional unit of Grs: molecular basis of CGA and ISQ sensing**
177 Ligand identification of insect Grs using heterologous expression systems (e.g., human cultural cells
178 and *Xenopus* oocytes) has often been unsuccessful and yielded little information. In the present study,
179 we identified some ligands of silkworm Grs. The EC_{50} value of BmGr9 to D-fructose from the present
180 study (aM level) is significantly lower than that previously reported by Sato *et al*. (mM level) [16]. They
181 did not observe BmGr9 response to D-glucose, sucrose, and *myo*-inositol up to 100 mM using calcium
182 imaging assay in the HEK293T cells [16]. Given that the detection sensitivity in our condition is much
183 higher because of the improvement of Gr expression levels and other unknown reasons, results from
184 Sato *et al.* and the present study were consistent. For instance, D-fructose exhibited the highest
185 affinity to BmGr9 among the tested sugars in our experiment (Fig. 2G), which was not inconsistent
186 with the negative results for D-glucose, sucrose, and *myo*-inositol in Sato *et al*. [16]. Meanwhile, the
187 CRISPR/Cas9-mediated KOs of BmGr6 and BmGr9 demonstrated that they could confer the MP

188 attomolar sensitivity to the mulberry compounds (Fig. 5) in partial agreement with the results from
189 calcium imaging using HEK293T cells (Fig. 2).
190 Our results confirm that single Gr can fully function as a receptor *in vitro*; nevertheless, it is evident
191 that heterologous expression of single Gr does not fully reconstitute its function *in vivo*. For example,
192 although BmGr6 served as a CGA receptor with attomolar sensitivity in HEK-293T cells (Fig. 2), the
193 KO of BmGr6 did not influence the MP sensitivity of CGA (Fig. 5). This is not due to functional
194 redundancy with other Grs, as the KO of BmGr9 resulted in a drastic decrease in CGA sensitivity (Fig.
195 5). It is possible that BmGr6 in MP neurons does not function as a homomeric complex but function
196 as a heteromeric complex by coupling with other Grs, as proposed in Ors in general and in some Grs
197 [32–35], resulting in different ligand spectra and sensitivity from the homomeric complex. Otherwise,
198 the difference in the expression levels and other factors between HEK293T cells and MP neurons
199 may affect the contribution of BmGr6 to the CGA sensitivity in MP neurons. Another example is that
200 both BmGr6 and BmGr9 are indispensable for ISQ sensing with attomolar sensitivity (Fig. 5),
201 suggesting a synergism between BmGr6 and BmGr9 to realize the attomolar sensitivity. In this case,
202 too, one possibility is that the two Grs couples in a functional heteromeric complex. Altogether, our
203 results suggest that BmGr6 and BmGr9 function as a heteromeric complex in MP neurons. Although
204 the heterologous expression of single Grs significantly contributed to the screening for Grs with
205 attomolar sensitivity to CGA and ISQ, its utility for dissecting *in vivo* molecular gustatory systems is
206 limited. We cannot rule out the possibility that Grs with lower sensitivities to CGA and ISQ than BmGr6
207 and BmGr9 *in vitro* are involved in attomolar sensing in MP by synergism with the two Grs. To
208 understand insect gustatory systems, it is required to decipher functional combinations of Grs and the
209 mechanism determining their ligand spectra.
210
211 **Putative fructose and sugar Grs in the silkworm act as plant phenolics receptors**
212 We demonstrate that BmGr6 and BmGr9 are responsible for ultrahigh-sensitive detection of CGA
213 and/or ISQ. The clades to which BmGr6 and BmGr9 belong are known as sugar receptor clades [29].
214 Nevertheless, we found that they are highly tuned to CGA and ISQ *in vitro* and responded to sugars
215 at relatively high concentrations (Fig. 2). As there was no drastic decrease in the feeding amount of
216 the artificial diet in BmGr6-KO and BmGr9-KO larvae in comparison with the WT (Fig. 4C), it is unlikely
217 that BmGr6 and BmGr9 also act as sucrose receptors in the MG. Unfortunately, we could not provide
218 direct evidence for that because we failed to record spikes from sugar-sensing neurons in the MG of
219 the N4 silkworm strains (both WT and mutants), probably because of their small amplitudes. Our data
220 suggest that the two Grs act as plant phenolics receptors rather than sugar receptors in silkworm
221 larvae's gustatory system. Phenolics are the most widely distributed plant secondary metabolites and
222 serve as stimulants and deterrents toward insects in feeding and oviposition [36]. Some Grs in the
223 putative sugar and fructose receptor clades may be receptors for plant phenolics which are
224 responsible for host plant selection in herbivorous insects.
225

The attomolar sensitivity is required for sensing leaf surface compounds in host plant selection

The experiments using BmGr6-KO and BmGr9-KO larvae provided further insights into the host recognition by MP. BmGr6-KO larvae lost their ability to sense ISQ but could still detect the remaining two essential compounds (CGA and β-sitosterol), inducing a test bite with the same ultrahigh sensitivity as the WT larvae (Fig. 5 and S3). Their low probability of test biting toward mulberry leaves (Fig. 4) confirmed the obligate authentication of the three compounds by MP. BmGr9-KO larvae have ~1,000-fold lower sensitivity toward CGA and ISQ. However, they exhibited high sensitivity even at the femtomolar level (Fig. 5), resulting in a lack of host recognition ability with high probability (Fig. 4E). This indicates that the femtomolar sensitivity is insufficient, and the attomolar sensitivity is required to sense leaf surface secondary compounds for host recognition. We recently showed silkworm MP's attomolar sensitivity toward feeding deterrents, such as coumarin and strychnine nitrate [37]. These ultrahigh sensitivities underlie feeding decisions by herbivorous larvae at the leaf surface.

In summary, we identified the two silkworms Grs responsible for the ultrahigh sensitivity in MP to sense leaf surface host phenolic compounds and recognize host leaves. Mechanistic insight into the gustatory system in herbivorous insects, especially on a functional unit of Grs, is needed to know how their Grs have adapted their tunings to plant secondary metabolites and their contribution to the evolution of feeding preferences.

Acknowledgments

The authors thank Shingo Kikuta (Ibaraki University) and Masataka G. Suzuki (The University of Tokyo) for technical assistance in calcium imaging at an early stage of this study and for establishing the CRISPR-Cas9 system. The Japan Society supported this research for the Promotion of Science (JSPS) KAKENHI (Grant Number 25660040 for RS; 18J00733 for HE).

Author contributions

H.E., K.T., and R.S. designed the research; H.E. and K.T. performed calcium imaging and electrophysiological recording studies; K.T. performed immunostaining and behavioral experiments; H.E., T.Y., and D.M. generated knockout mutants under the supervision of K.I. and S.N. H.E. wrote the manuscript with intellectual inputs from all authors.

Conflict of interest

The authors declare no conflicts of interest.

Material and methods

Insect rearing

The silkworm *Bombyx mori* larvae (N4 strain and Kinshu × Showa hybrid) were reared at 25°C on an artificial diet Silkmate 2M (Nihon-Nosan Co. Ltd.) under a 12 h light–12 h dark photoperiod. The N4

264 larvae were used for experiments in Fig. 2, 4, 5, S3, and S4. The Kinshu × Showa larvae were used
265 for immunostaining in Fig. 3.
266
267 **Phylogenetic analysis**
268 The lepidopteran Gr phylogeny was generated using full-length amino acid sequences of Grs from
269 *Bombyx mori* [30], *P. xylostella* [38], *H. melpomene* [39], PxutGr1 [23], and PrapGr28 [24]. The
270 sequences were aligned with MAFFT v.7 (http://mafft.cbrc.jp/alignment/server/). The IQ-TREE web
271 server (http://iqtree.cibiv.univie.ac.at/) generated the maximum-likelihood tree using the JTT+F+I+G4
272 model. The phylogenetic tree was visualized using iTOL (https://itol.embl.de/) [40].
273
274 **cDNA cloning of *Bombyx* Grs**
275 cDNA of BmGr6, BmGr7, BmGr9, and BmGr10 were cloned into the pcDNA3.1 vector (Thermo Fisher
276 Scientific) as reported previously [19,41]. According to the nucleotide sequences reported by Guo *et*
277 *al*. [30], cDNA of BmGr4, BmGr5, and BmGr8 were codon-optimized for mammalian cell expression,
278 artificially synthesized (gBlocks®, Integrated DNA Technologies), and inserted into the EcoRV site of
279 pcDNA3.1 vector using GeneArt® Seamless Cloning and Assembly Enzyme Mix (Thermo Fisher
280 Scientific).
281
282 **Cell culture and transfection**
283 HEK293T cells were cultured in Dulbecco's modified Eagle medium (DMEM, Thermo fisher scientific)
284 supplemented with 10% fetal bovine serum (BioWest), 4 mM GlutaMAX (Thermo Fisher Scientific),
285 100 units/ml penicillin (Meiji Seika Pharma Co., Ltd.), and 100 mg/ml streptomycin (Meiji Seika
286 Pharma Co., Ltd.) with 5% CO_2 at 37°C. For preparing transfection solutions, 500 μL Opti-MEM
287 (Thermo Fisher Scientific) were vortexed with 4–6 μg polyethylenimine (PEI Max, Polysciences, Inc.,
288 Warrington, PA) and incubated for 5 min. Afterward, 2 μg of an expression vector was added, vortexed
289 vigorously, and incubated for 20 min. Approximately 50%–70% confluent HEK293T cells were seeded
290 on a coverslip in a six-well plate and transfected with the transfection solution for 4 h with 5% CO_2 at
291 37°C. The media was replaced with DMEM, and the cells were incubated for 48 h.
292
293 **Calcium imaging**
294 For preparing the loading solution of Ca^{2+} indicator Fluo-4 AM (Thermo Fisher Scientific), 3 μL of
295 1 mM Fluo-4 AM (stock solution in DMSO) and 30 μL of PowerLoad Concentrate (100X, Thermo
296 Fisher Scientific) were vortexed vigorously. The mixture (5 μL) was added into a six-well plate
297 containing 500 μL Hank's buffered saline solution (HBSS, 137 mM NaCl, 5.4 mM KCl, 0.3 mM
298 Na_2HPO_4, 0.4 mM KH_2PO_4, 4.2 mM $NaHCO_3$, 1.3 mM $CaCl_2$, 0.5 mM $MgCl_2$, and 0.4 mM $MgSO_4$, pH
299 7.4) incubated for 10 min at 37°C (final conc. ~1 μM Fluo4-AM and ~1X PowerLoad). After loading,
300 the solution was replaced with HBSS containing 0.75 mM Probenecid (Thermo Fisher Scientific). After
301 1 h incubation, the cells were used for calcium imaging experiments.

302 Calcium imaging was performed with a flow system under the fluorescence microscope BX53
303 (Olympus) equipped with a MetaView imaging system (Molecular Devices). A coverslip on which
304 transfected cells were seeded was inverted and put on a self-manufactured chamber with a 5-mm-
305 wide flow channel. A ligand dissolved in HBSS was superfused at a proper flow rate with peristaltic
306 pumps (PERISTA pump, ATTO). CGA (Nacalai tesque, Kyoto, Japan), ISQ (Extrasynthese, Lyon,
307 France), D-glucose, D-fructose, sucrose, and *myo*-inositol (Fujifilm Wako Pure Chemical Corp.,
308 Osaka, Japan) were directly dissolved in HBSS. β-sitosterol (Abcam, Cambridge, UK) was dissolved
309 in a 45% solution of 2-hydroxypropyl-β-cyclodextrin at 37°C to prepare stable aqueous solutions. The
310 time-lapsed fluorescence images (1 Hz) were processed using Fiji [42], and the fluorescent ratio
311 (ΔF/F) was calculated as peak intensity divided by basal intensity (mean of 10 flames before ligand
312 perfusion). The EC_{50} value was calculated by fitting using the four-parameter logistic model (Prism
313 ver.8, Graph-Pad).
314
315 **Immunostaining**
316 The heads of the fifth instar larvae (Kinshu × Showa hybrid) were fixed with 4%
317 paraformaldehyde/phosphate-buffered saline (PBS, 137 mM NaCl, 2.7 mM KCl, 10 mM Na_2HPO_4,
318 1.8 mM KH_2PO_4, pH 7.4) overnight at 4°C. The fixed heads were dissected, and the maxilla was
319 collected and immersed into a cryoprotection solution (10% sucrose/PBS at room temperature (RT)
320 for 3 h; 20% sucrose/PBS at 4°C overnight; 30% sucrose/PBS at 4°C overnight), embedded in Tissue-
321 Tek O.C.T. Compound (Sakura Finetek Japan Co., Ltd) and stored at −80°C. The embedded
322 specimens were sectioned at 14 μm thickness via cryostat (CM3050S, Leica, Wetzlar, Germany),
323 mounted on the coated slide glasses (MAS-03, Matsunami Glass, Osaka, Japan), and air dried at RT
324 for a day. After 5 min washes with Tris-NaCl-Tween buffer (TNT; 0.15 M Tris-HCl, 0.01 M NaCl, 0.05%
325 Tween20), the sections were permeabilized with 0.1% TritonX-100/TNT for 5–10 min, blocked with
326 2% bovine serum albumin (BSA)/TNT for 30 min, and incubated with primary antiserum raised
327 elsewhere [41,43] (anti-BmGr6 and anti-BmGr9 antisera in 2% BSA/TNT at a 1:100 dilution) for 12 h
328 at 4°C. After three 5 min washes with TNT, the sections were incubated in a secondary antiserum (an
329 antimouse IgG conjugated with Alexa Fluor 488, Molecular Probes, USA), at a 1:1,000 dilution in TNT
330 for 12 h at 4°C. After three TNT washes for 5 min, the sections were counterstained with 4, 6-
331 diamidino-2-phenylindole (l mg/mL, Sigma Aldrich, Schnelldorf, Germany) for 5 min at RT. After 5 min
332 of TNT wash, the sections were mounted in 90% glycerol/PBS containing 1, 4-diazabicyclo[2.2.2]
333 octane at RT and observed under fluorescence microscopy (BX53, Olympus, Tokyo, Japan).
334
335 **Generation of Gr-KO silkworm strains using CRISPR/Cas9 genome editing**
336 We used the Alt-R® CRISPR-Cas9 system (Integrated DNA Technologies) to generate silkworm
337 strains carrying null mutations in *BmGr6* or *BmGr9* genes. CRISPRdirect (Naito *et al*., 2015) identified
338 unique target sequences for guide RNAs using *Bombyx mori* genome assembly as a reference. Alt-
339 R® crRNAs (for BmGr6: 5′-GTATTCGGCGGCGCTGGGAATGG-3′; for BmGr9, 5′-

340 CTGGTGGCGGAGATAGGAGTGGG-3′), tracrRNA, and S.p. Cas9 Nuclease V3 were purchased
341 from Integrated DNA Technologies. CRISPR-Cas9 ribonucleoprotein (RNP) complexes containing 10
342 μM crRNA:tracrRNA duplex and 300 ng/μL Cas9 enzyme were prepared according to a user-
343 submitted protocol entitled "CRISPR-Cas9 RNP delivery—*B. tryoni* microinjection—A Choo" on the
344 Integrated DNA Technologies website. Newly laid eggs of the WT N4 strain were aligned and glued
345 onto a sliding glass, and RNP complexes were injected using IM 300 Microinjector (NARISHIGE)
346 within 5–8 h after oviposition. Generation 0 (G_0) moths were crossed with WT moths. To identify
347 Generation 1 (G_1) broods carrying a heterozygous Cas9-induced mutation, genomic DNA extracted
348 from ~10 G_1 eggs were used for the T7 Endonuclease I (T7EI) assay with Alt-R® Genome Editing
349 Detection Kit (Integrated DNA Technologies). T7EI assay-positive G_1 moths were subjected to sibling
350 mating or crossed with WT moths. Mutations were identified by DNA sequencing of genomic PCR
351 (gPCR) products. Mutant strains carrying a homozygous null mutation were generated by
352 intercrossing G_2 or G_3 moths.
353
354 **Feeding behavior assays**
355 The feeding behavior assays were performed as described previously [8]. For feeding assay, three to
356 five fifth instar larvae (Day 0) were put on individual Petri dishes, and the larval mass before and after
357 1.5 h feeding was measured. An increase in larval mass was regarded as the amount of food intake
358 because no feces were observed after feeding. We adopted an increase in body mass (%, w/w) as
359 the index of food intake because a significant correlation between the amount of food intake and the
360 original body mass was observed via Pearson's correlation analysis (Fig. S4). Mulberry leaves were
361 collected around the campus of the Tokyo University of Agriculture and Technology (Koganei, Tokyo,
362 Japan) and stored at 4°C. To observe test bites, videos of silkworm feeding on leaves were captured
363 by a D5100 camera (Nikon, Tokyo, Japan) equipped with a telephoto lens AF-S DX Micro Nikkor 85
364 mm (Nikon, Tokyo, Japan). The larvae were used 24–48 h after molting to the fifth instar. To prevent
365 nonspecific biting due to starvation, all larvae were fed on artificial diets for 2 min before use.
366
367 **Tip recording**
368 Tip recording was performed as described previously [8]. In brief, the heads of the fifth instar larvae
369 (Day 0) were excised and used for further experiments within ~20 min. The whole sensilla of MP were
370 capped with a glass capillary (Erma Inc., Tokyo, Japan) filled with a tastant solution dissolved in 5
371 mM NaCl using a micromanipulator (NARISHIGE, Tokyo, Japan). Electrical signals were amplified by
372 a TastePROBE amplifier (Syntech, Hilversum, The Netherlands), recorded via PowerLab 2/25 (AD
373 Instruments, Sydney, Australia), and analyzed by the LabChart software (AD Instruments). Spikes
374 were counted from 0.1 to 1.1 s after the onset of stimulation using custom codes written in MATLAB
375 (Mathworks). Thresholds for counting spikes were set from 3 to 10 mV depending on the baseline
376 amplitude.

377

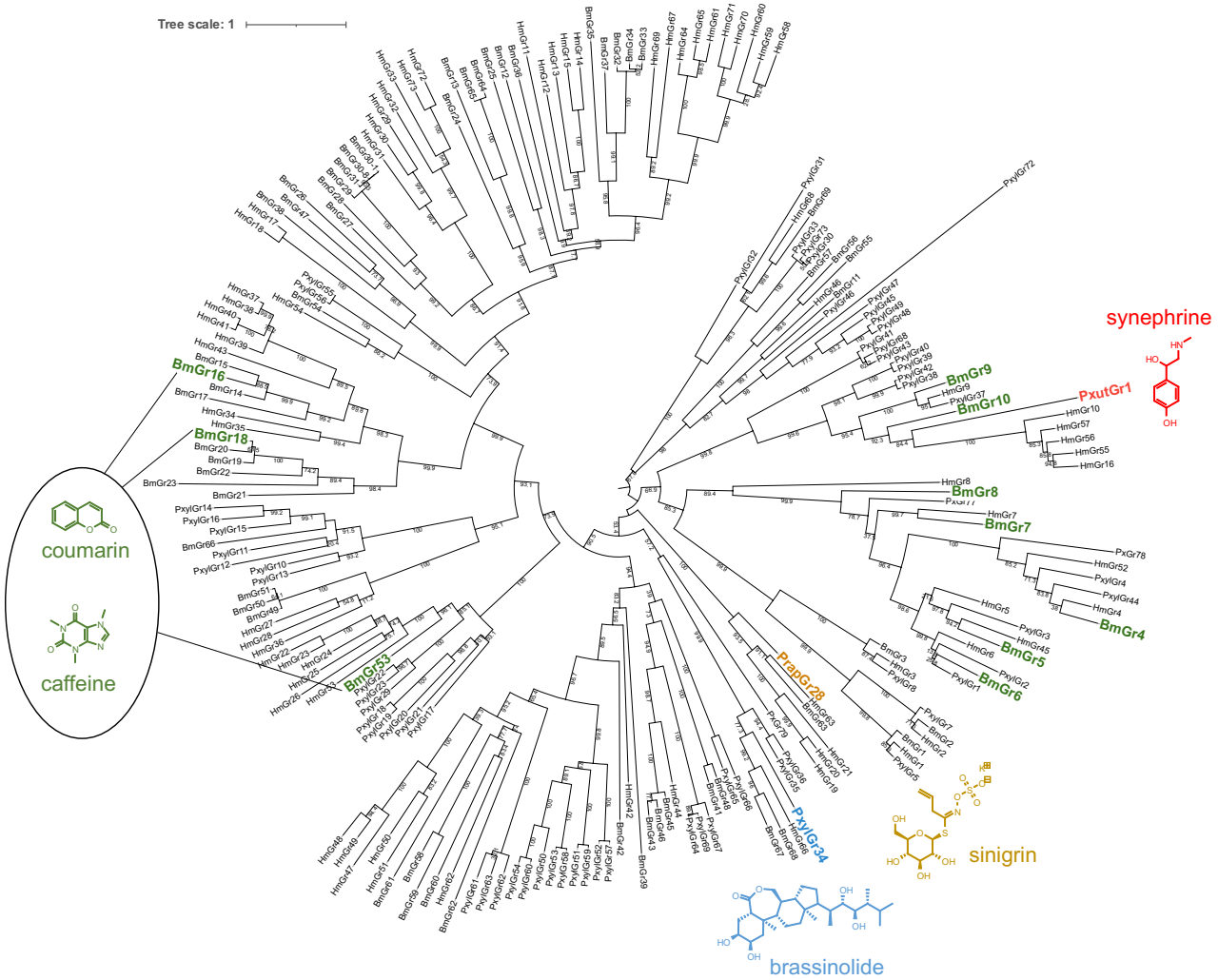

378

379 **Fig. 1. Phylogeny of the gustatory receptors in some lepidopteran insects.** The combination of
380 gustatory receptors and plant secondary metabolites as their ligands were highlighted with the same
381 colors as reported in previous studies [23,24,26,27]. Bm: *B. mori* [30]; Pxyl: *P. xylostella* [38]; Hmel:
382 *H. melpomene* [39].

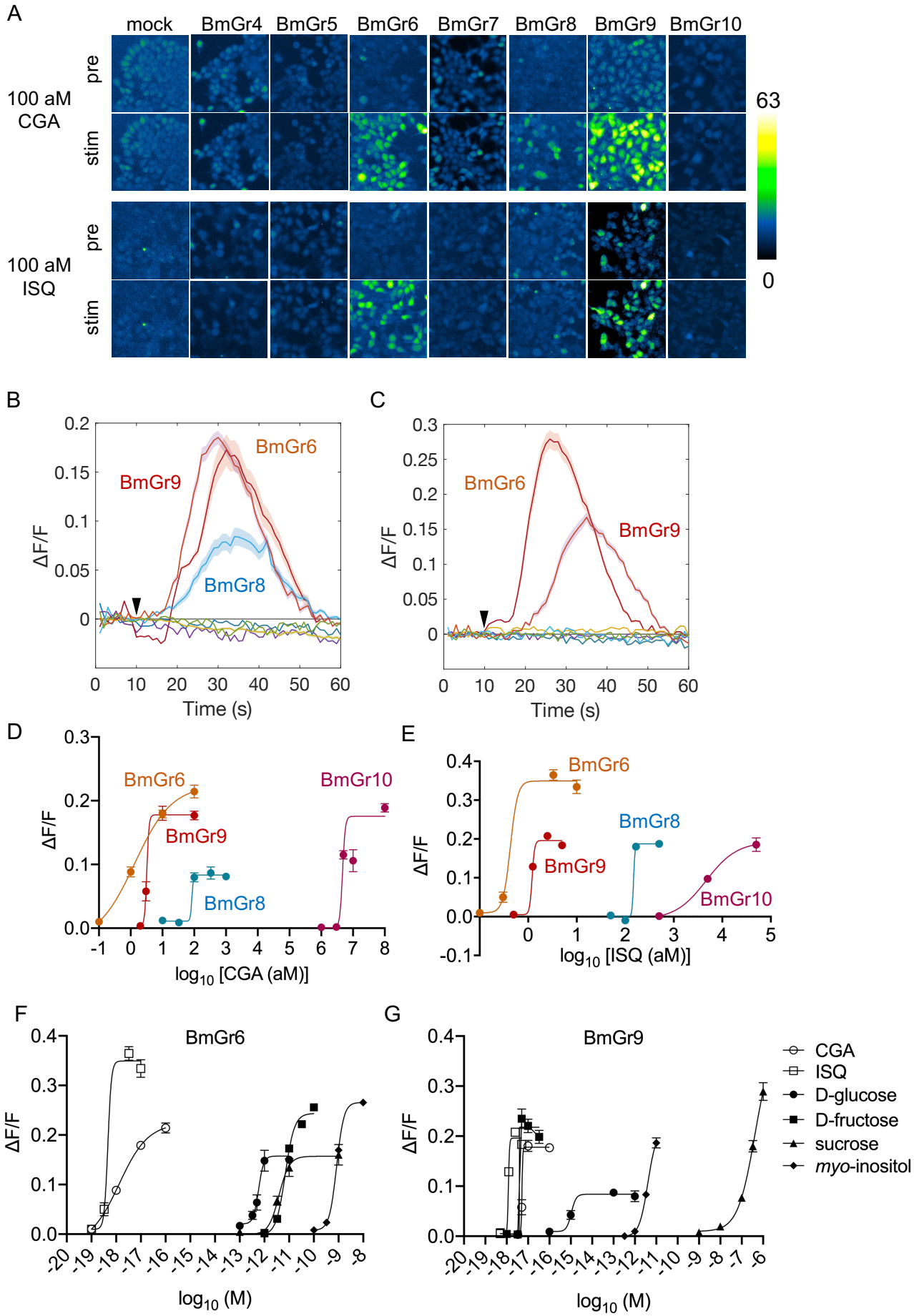
A
mock
BmGr4
BmGr5
BmGr6
BmGr7
BmGr8
BmGr9
BmGr10
100 aM CGA
pre
stim
100 aM ISQ
pre
stim
63
0
B
BmGr6
BmGr9
BmGr8
ΔF/F
Time (s)
C
BmGr6
BmGr9
ΔF/F
Time (s)
D
BmGr6
BmGr9
BmGr8
BmGr10
ΔF/F
log10 [CGA (aM)]
E
BmGr6
BmGr8
BmGr9
BmGr10
ΔF/F
log10 [ISQ (aM)]
F
BmGr6
ΔF/F
log10 (M)
G
BmGr9
ΔF/F
log10 (M)
CGA
ISQ
D-glucose
D-fructose
sucrose
myo-inositol

383

Fig. 2. Calcium imaging of BmGrs-expressing HEK293T cells. (A) The response of BmGr-expressing cells to 100 aM chlorogenic acid (CGA) and isoquercitrin (ISQ). The representative cell images before (pre) and after (stim) stimulation. Fluorescent intensity is color-coded according to the scale bar. (B and C) Time course of responses (ΔF/F) toward 100 aM CGA (B) and ISQ (C) (n = 30). The arrowheads indicate the timing of the ligand application. (D and E) Dose-dependent responses of BmGr6, BmGr8, BmGr9, and BmGr10 toward CGA (D) and ISQ (E). (F and G) Dose-dependent responses of BmGr6 (F) and BmGr9 (G) toward CGA, ISQ, and sugars (B–G). Data are represented as the mean ± SEM.

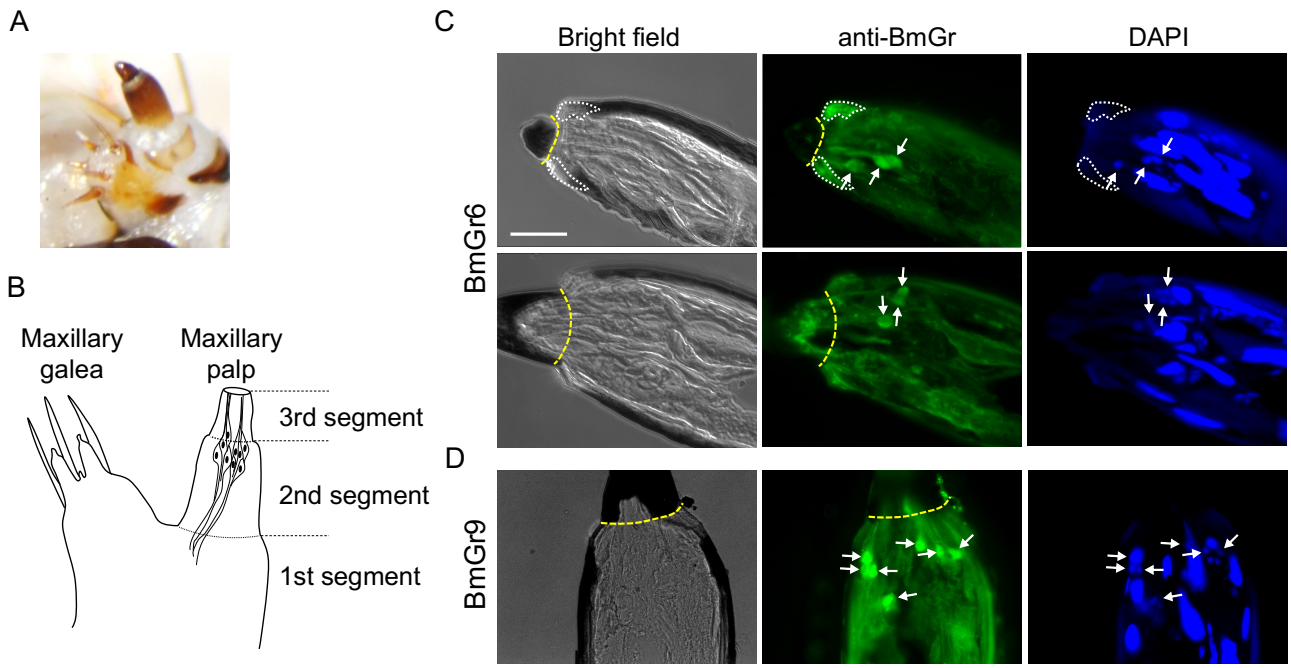

Fig. 3. Immunostaining using maxillary palp (MP) BmGr6 and BmGr9 antibodies. (A and B) Image (A) and schematic diagram (B) of the maxilla of a silkworm larva. (C and D) Expression of BmGr6 (C) and BmGr9 (D). Arrows indicate somas of immunoreactive sensory neurons. The areas surrounded by broken white lines indicate the autofluorescence of the cuticle. Yellow broken lines indicate the border between MP's second and third segments. Scale bar: 25 μm.

A

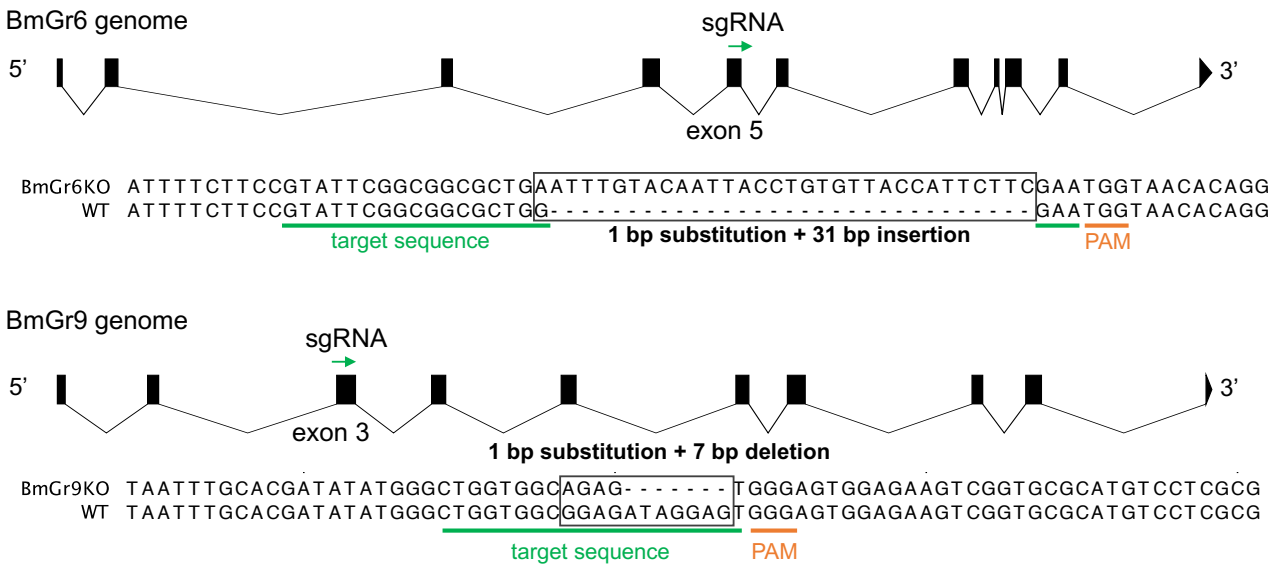
BmGr6 genome
sgRNA
5'
3'
exon 5
BmGr6KO ATTTTCTTCCGTATTCGGCGGCGCTGAATTTGTACAATTACCTGTGTTACCATTCTTCGAATGGTAACACAGG
WT ATTTTCTTCCGTATTCGGCGGCGCTGG- - - -

400 **Fig. 4. Generation and characterization of BmGr6-KO and BmGr9-KO larvae.** (A) Gene structures,
401 sgRNA target sites, including the adjacent protospacer motif (PAM), and obtained CRISPR/Cas9-
402 mediated mutations of *BmGr6* and *BmGr9*. Gene structures were drawn using Exon-Intron Graphic
403 Maker (http://wormweb.org/exonintron). (B) The body mass of freshly molted larvae (Day 0 of the fifth
404 instar) (n = 140–175). (C and D) The increase in larval body mass after 1.5 h feeding of artificial diets
405 (C) (n = 75–117) and mulberry leaves (D) (n = 60). (E) The proportion of larvae showing test biting
406 toward mulberry leaves. The biting of ten larvae was observed for one minute. Experiments were
407 repeated as independent biological replicates (n = 7–11). (F) Palpation time until the first bite toward
408 mulberry leaves (n = 23–99). Data are represented as the mean ± SEM. Statistical analysis was
409 performed by one-way ANOVA followed by the Tukey post hoc test. “ns” indicates no significant
410 difference; an asterisk indicates a significant difference (**$P < 0.01$; ****$P < 0.0001$).

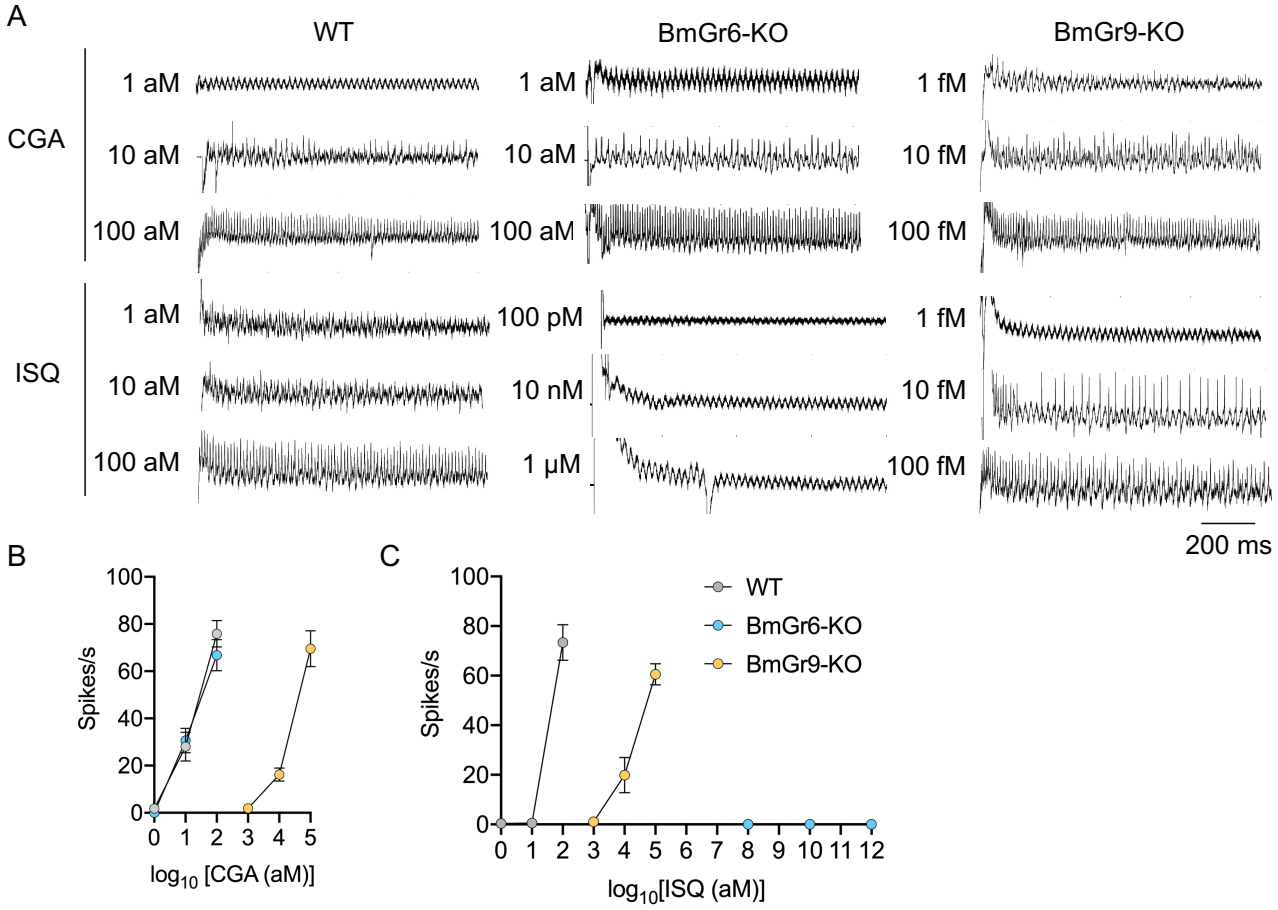

Fig. 5. Electrophysiological recordings of the maxillary palp (MP) in BmGr6-KO and BmGr9-KO larvae. The representative traces (A) and frequencies of action potentials from the whole MP sensilla in response to chlorogenic acid (CGA) (B) and isoquercitrin (ISQ) (C). Spikes were counted from 0.1 to 1.1 s after the onset of stimulation. Error bars are represented as SEM (n = 6–8).

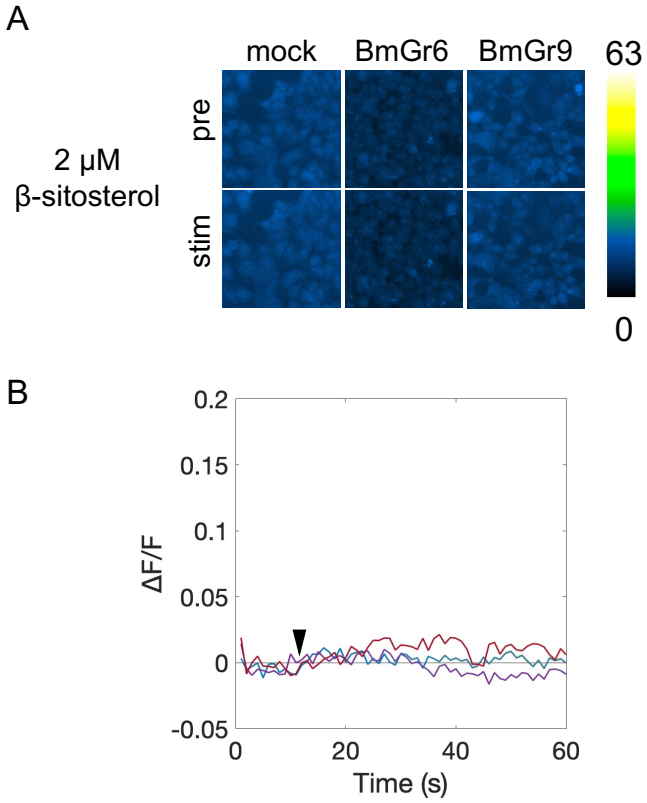

Fig. S1. Response of BmGr6- and BmGr9-expressing cells toward β-sitosterol. (A) The representative cell images before (pre) and after (stim) stimulation by 2 μM β-sitosterol. Fluorescent intensity is color-coded according to the scale bar. (B) Time course of responses (ΔF/F) toward 2 μM β-sitosterol (n = 30). The arrowhead indicates the timing of the ligand application.

A

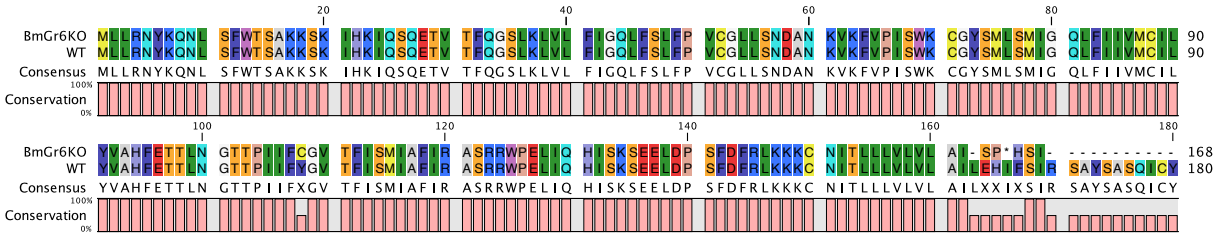

B

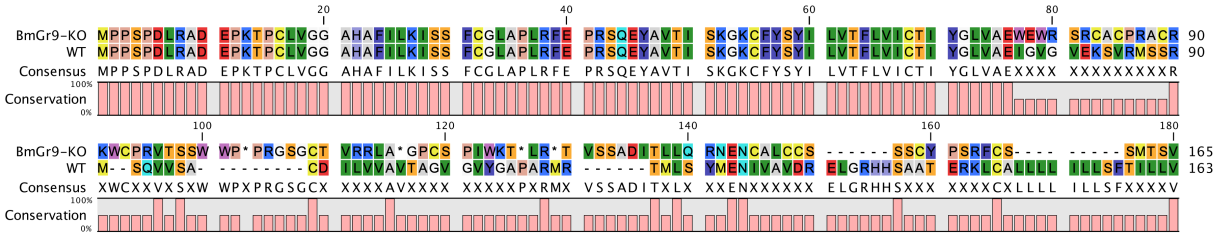

Fig. S2. Deduced amino acid sequences of truncated BmGr6 (A) and BmGr9 (B) in knockout larvae. The sequences were aligned using CLC Sequence Viewer 8 (CLC Bio, Aarhus, Denmark).

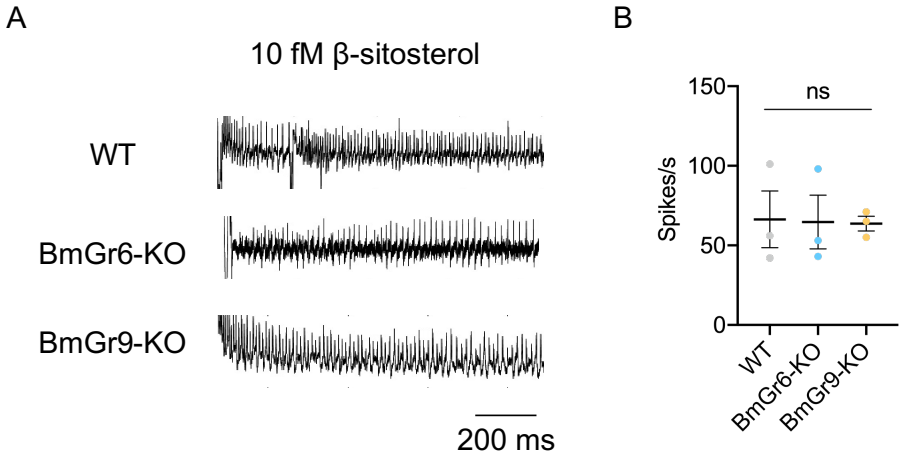

Fig. S3. Response of the maxillary palp (MP) in BmGr6-KO and BmGr9-KO larvae toward β-sitosterol. The representative traces (A) and frequencies of action potentials from the whole MP sensilla in response to 10 fM β-sitosterol (B). Spikes were counted from 0.1 to 1.1 s after the onset of stimulation. Data are represented as the mean ± SEM (n = 3). Statistical analysis was performed via one-way ANOVA followed by the Tukey post hoc test. “ns” indicates no significant difference.

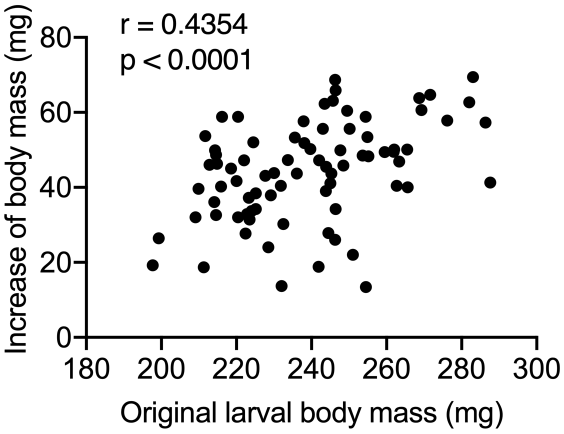

Fig. S4. Correlation between original body mass and feeding amount. Correlation coefficient (r) using Pearson correlation analysis (n = 80).

434 **Table S1. EC_{50} values of BmGrs in response to plant secondary metabolites (chlorogenic acid**
435 **(CGA) and isoquercitrin (ISQ)) and sugars.**

Gr	BmGr6	BmGr8	BmGr9	BmGr10	BmGr6	BmGr8	BmGr9	BmGr10
ligand	CGA	CGA	CGA	CGA	ISQ	ISQ	ISQ	ISQ
IC50 (aM)	1.329	~ 84.55	~ 3.226	4692479	~ 0.4287	~ 148.4	~ 1.205	4663

Gr	BmGr6	BmGr6	BmGr6	BmGr6	BmGr9	BmGr9	BmGr9	BmGr9
ligand	D-glucose	D-fructose	sucrose	myo-inositol	D-glucose	sucrose	D-fructose	myo-inositol
IC50 (M)	5.778E-13	6.993E-12	3.909E-12	8.378E-10	~ 1.059e-015	4.198E-07	~ 3.903e-018	4.051E-12

436

437 **References**

438 1. War AR, Paulraj MG, Ahmad T, Buhroo AA, Hussain B, Ignacimuthu S, et al. Mechanisms of
439 plant defense against insect herbivores. Plant Signal Behav. 2012;7: 1306–1320.
440 2. Fraenkel GS. The Raison d'Être of Secondary Plant Substances. Science. 1959;129: 1466–
441 1470.
442 3. Heidel-Fischer HM, Vogel H. Molecular mechanisms of insect adaptation to plant secondary
443 compounds. Curr Opin Insect Sci. 2015;8: 8–14.
444 4. Simon J-C, d'Alençon E, Guy E, Jacquin-Joly E, Jaquiéry J, Nouhaud P, et al. Genomics of
445 adaptation to host-plants in herbivorous insects. Brief Funct Genomics. 2015;14: 413–423.
446 5. Chapman RF. Contact chemoreception in feeding by phytophagous insects. Annu Rev
447 Entomol. 2003;48: 455–484.
448 6. Chapman RF, Bernays EA. Insect behavior at the leaf surface and learning as aspects of host
449 plant selection. Experientia. 1989;45: 215–222.
450 7. Renwick JAA. Chemical ecology of oviposition in phytophagous insects. Experientia. 1989;45:
451 223–228.
452 8. Tsuneto K, Endo H, Shii F, Sasaki K, Nagata S, Sato R. Diet choice: The two-factor host
453 acceptance system of silkworm larvae. PLoS Biol. 2020;18: e3000828.
454 9. Cheng D, Mulder PPJ, van der Meijden E, Klinkhamer PGL, Vrieling K. The correlation between
455 leaf-surface and leaf-tissue secondary metabolites: a case study with pyrrolizidine alkaloids in
456 Jacobaea hybrid plants. Metabolomics. 2017;13: 47.
457 10. Chun MW. Dynamics of Feeding Responses in Pieris brassicae Linn. as a Function of
458 Chemosensory Input: A Behavioural, Ultrastructural and Electrophysiological Study. de Wilde J,
459 editor. Wageningen University and Research. 1972. Available:
460 https://library.wur.nl/WebQuery/wurpubs/421851
461 11. Devitt BD, Smith JJB. ACTION OF MOUTHPARTS DURING FEEDING IN THE DARK-SIDED
462 CUTWORM, EUXOA MESSORIA (LEPIDOPTERA: NOCTUIDAE). Can Entomol. 1985;117:
463 343–349.
464 12. Montell C. Drosophila sensory receptors-a set of molecular Swiss Army Knives. Genetics.
465 2021;217: 1–34.
466 13. Slone J, Daniels J, Amrein H. Sugar receptors in Drosophila. Curr Biol. 2007;17: 1809–1816.
467 14. Dahanukar A, Lei Y-T, Kwon JY, Carlson JR. Two Gr genes underlie sugar reception in
468 Drosophila. Neuron. 2007;56: 503–516.
469 15. Chyb S, Dahanukar A, Wickens A, Carlson JR. Drosophila Gr5a encodes a taste receptor
470 tuned to trehalose. Proc Natl Acad Sci U S A. 2003;100 Suppl 2: 14526–14530.
471 16. Sato K, Tanaka K, Touhara K. Sugar-regulated cation channel formed by an insect gustatory
472 receptor. Proc Natl Acad Sci U S A. 2011;108: 11680–11685.
473 17. Miyamoto T, Slone J, Song X, Amrein H. A fructose receptor functions as a nutrient sensor in
474 the Drosophila brain. Cell. 2012;151: 1113–1125.

18. Zhang H-J, Anderson AR, Trowell SC, Luo A-R, Xiang Z-H, Xia Q-Y. Topological and functional characterization of an insect gustatory receptor. PLoS One. 2011;6: e24111.
19. Kikuta S, Endo H, Tomita N, Takada T, Morita C, Asaoka K, et al. Characterization of a ligand-gated cation channel based on an inositol receptor in the silkworm, Bombyx mori. Insect Biochem Mol Biol. 2016;74: 12–20.
20. Dweck HKM, Carlson JR. Molecular Logic and Evolution of Bitter Taste in Drosophila. Curr Biol. 2020;30: 17-30.e3.
21. Steck K, Walker SJ, Itskov PM, Baltazar C, Moreira J-M, Ribeiro C. Internal amino acid state modulates yeast taste neurons to support protein homeostasis in Drosophila. Elife. 2018;7. doi:10.7554/eLife.31625
22. Tauber JM, Brown EB, Li Y, Yurgel ME, Masek P, Keene AC. A subset of sweet-sensing neurons identified by IR56d are necessary and sufficient for fatty acid taste. PLoS Genet. 2017;13: e1007059.
23. Ozaki K, Ryuda M, Yamada A, Utoguchi A, Ishimoto H, Calas D, et al. A gustatory receptor involved in host plant recognition for oviposition of a swallowtail butterfly. Nat Commun. 2011;2: 542.
24. Yang J, Guo H, Jiang N-J, Tang R, Li G-C, Huang L-Q, et al. Identification of a gustatory receptor tuned to sinigrin in the cabbage butterfly Pieris rapae. PLoS Genet. 2021;17: e1009527.
25. Renwick JAA, Lopez K. Experience-based food consumption by larvae of Pieris rapae : addiction to glucosinolates? Entomol Exp Appl. 1999;91: 51−58.
26. Yang K, Gong X-L, Li G-C, Huang L-Q, Ning C, Wang C-Z. A gustatory receptor tuned to the steroid plant hormone brassinolide in Plutella xylostella (Lepidoptera: Plutellidae). Elife. 2020;9. doi:10.7554/eLife.64114
27. Kasubuchi M, Shii F, Tsuneto K, Yamagishi T, Adegawa S, Endo H, et al. Insect taste receptors relevant to host identification by recognition of secondary metabolite patterns of non-host plants. Biochem Biophys Res Commun. 2018;499: 901–906.
28. Liu X-L, Zhang J, Yan Q, Miao C-L, Han W-K, Hou W, et al. The Molecular Basis of Host Selection in a Crucifer-Specialized Moth. Curr Biol. 2020;30: 4476-4482.e5.
29. Wanner KW, Robertson HM. The gustatory receptor family in the silkworm moth Bombyx mori is characterized by a large expansion of a single lineage of putative bitter receptors. Insect Mol Biol. 2008;17: 621–629.
30. Guo H, Cheng T, Chen Z, Jiang L, Guo Y, Liu J, et al. Expression map of a complete set of gustatory receptor genes in chemosensory organs of Bombyx mori. Insect Biochem Mol Biol. 2017;82: 74–82.
31. Asaoka. Ultrastructure of maxillary sensilla in the silkworm, Bombyx mori: differences among strains? J Insect Biotechnol Sericology. 2003. Available: https://www.jstage.jst.go.jp/article/jibs/72/2/72_2_117/_article/-char/ja/

513 32. Vosshall LB, Amrein H, Morozov PS, Rzhetsky A, Axel R. A spatial map of olfactory receptor
514 expression in the Drosophila antenna. Cell. 1999;96: 725–736.
515 33. Del Mármol J, Yedlin MA, Ruta V. The structural basis of odorant recognition in insect olfactory
516 receptors. Nature. 2021. doi:10.1038/s41586-021-03794-8
517 34. Jiao Y, Moon SJ, Wang X, Ren Q, Montell C. Gr64f is required in combination with other
518 gustatory receptors for sugar detection in Drosophila. Curr Biol. 2008;18: 1797–1801.
519 35. Shim J, Lee Y, Jeong YT, Kim Y, Lee MG, Montell C, et al. The full repertoire of Drosophila
520 gustatory receptors for detecting an aversive compound. Nat Commun. 2015;6: 8867.
521 36. Singh S, Kaur I, Kariyat R. The Multifunctional Roles of Polyphenols in Plant-Herbivore
522 Interactions. Int J Mol Sci. 2021;22. doi:10.3390/ijms22031442
523 37. Shii F, Mang D, Kasubuchi M, Tsuneto K, Toyama T, Endo H, et al. Ultrasensitive detection by
524 maxillary palp neurons allows non-host recognition without consumption of harmful
525 allelochemicals. J Insect Physiol. 2021;132: 104263.
526 38. Engsontia P, Sangket U, Chotigeat W, Satasook C. Molecular evolution of the odorant and
527 gustatory receptor genes in lepidopteran insects: implications for their adaptation and
528 speciation. J Mol Evol. 2014;79: 21–39.
529 39. Briscoe AD, Macias-Muñoz A, Kozak KM, Walters JR, Yuan F, Jamie GA, et al. Female
530 behaviour drives expression and evolution of gustatory receptors in butterflies. PLoS Genet.
531 2013;9: e1003620.
532 40. Letunic I, Bork P. Interactive Tree Of Life (iTOL) v5: an online tool for phylogenetic tree display
533 and annotation. Nucleic Acids Res. 2021;49: W293–W296.
534 41. Mang D, Shu M, Endo H, Yoshizawa Y, Nagata S, Kikuta S, et al. Expression of a sugar clade
535 gustatory receptor, BmGr6, in the oral sensory organs, midgut, and central nervous system of
536 larvae of the silkworm Bombyx mori. Insect Biochem Mol Biol. 2016;70: 85–98.
537 42. Schindelin J, Arganda-Carreras I, Frise E, Kaynig V, Longair M, Pietzsch T, et al. Fiji: an open-
538 source platform for biological-image analysis. Nat Methods. 2012;9: 676–682.
539 43. Mang D, Shu M, Tanaka S, Nagata S, Takada T, Endo H, et al. Expression of the fructose
540 receptor BmGr9 and its involvement in the promotion of feeding, suggested by its co-
541 expression with neuropeptide F1 in *Bombyx mori*. Insect Biochem Mol Biol. 2016;75: 58-69.